

Ionic Conductivities of the LiCF_3SO_3 Complexes with Liquid Crystalline Aromatic Polyesters Having Oligo(oxyethylene) Pendants

Jun-Woo Lee, Sung-Hoon Joo, and Jung-Il Jin*

Division of Chemistry and Molecular Engineering and Center for Electro- and Photo-Responsive Molecules,
Korea University, Seoul 136-701, Korea

Received September 19, 2003; Revised March 8, 2004

Abstract: We have synthesized new aromatic polyesters (DiPEG-HQ and DiPEG-BP) by condensation polymerization of a terephthalic acid derivative bearing a pendant oligo(oxyethylene) ($\overline{DP} = 7$, $MW = 350$), which has a methoxy terminal group, and two different aromatic diols, hydroquinone and 4,4'-biphenol. The synthesized polymers were characterized by differential scanning calorimetry (DSC), polarizing microscopy, and X-ray diffractometry for their liquid crystallinity (LC), thermal transitions, and structural morphologies in mesophases. The morphology of the LC phases depends strongly on the length of the rigid backbone repeating unit. The DiPEG-BP polymer having a longer repeating unit exhibits both layered and nematic structures before isotropization, whereas the DiPEG-HQ polymer having a shorter repeating unit shows only the layered structure in the mesophase. We found that the layer spacing for DiPEG-HQ is larger than that for DiPEG-BP. Both polymers easily form complexes with LiCF_3SO_3 ; we studied this complex formation by FT-IR spectroscopy. The layer spacing of the polymer-electrolyte composites increases upon increasing the amount of the lithium salt. The polymer/salt electrolyte mixtures we investigated at molar ratios of EO:salt in the range of 5-20 exhibit electrical conductivity values at 40 °C of 2.4×10^{-5} and 1.1×10^{-5} S/cm for DiPEG-HQ/ LiCF_3SO_3 and DiPEG-BP/ LiCF_3SO_3 , respectively. At 80 °C, these values are higher: 4.6×10^{-4} and 2.5×10^{-4} S/cm, respectively. The activation energy of conductivity depends strongly on the salt concentration.

Keywords: ionic conductivity, LC aromatic polyester, oligo(oxyethylene), pendants, LiCF_3SO_3 , complexes.

Introduction

In recent years, solid polymer electrolytes (SPE) have been extensively studied due to their potential applications,¹⁻⁷ particularly for the development of high-energy density batteries.⁸⁻¹⁰ Among those, poly(ethylene oxide) (PEO)-based electrolytes are the most extensively studied. In PEO/alkali complexes, ionic conduction is limited to the amorphous regions and the inherent high crystallizability of PEO is known to be a main reason for the relatively poor ionic conductivities.¹¹⁻¹⁵

Many investigations have therefore focused primarily on the enhancement of the room-temperature conductivity taking various approaches such as using blends,¹⁶⁻¹⁹ random copolymers,²⁰ and comb-branch polymers.²¹⁻²⁴ All these approaches have been focused on reducing the crystallinity of polymers. Among other classes of polymers studied, poly((methoxyethoxy) ethoxyphosphazene) (MEEP)^{23,24} having

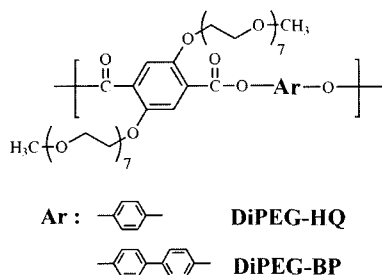
a highly flexible backbone, reveals a high mobility of complexed ions. The conductivity of MEEP-based electrolytes was reported to be in the range of 10^{-4} - 10^{-5} S/cm at room temperature. Very recently, Heo *et al.*²⁵ reported that the maximum conductivity of a lithium *p*-[methoxyoligo(oxyethylene)] benzenesulfonates reached about 5×10^{-4} Scm^{-1} at room temperature.

However, most of the reported polymers have a disadvantage of poor mechanical properties. Recently, there have been several synthetic attempts to improve the mechanical strength of SPEs. Ward *et al.*²⁶ and other researchers²⁷⁻²⁹ reported that the main chain liquid crystalline polymers (LCPs) containing PEO moieties can be obtained by inserting mesogenic groups into the ionically conducting polymer backbone. On the other hand, Wegner *et al.*³⁰ studied electrical properties of alkali salt-doped stiff main chain macromolecules bearing flexible oligo(oxyethylene) side pendants. Recently, we³¹ briefly reported synthesis and characterization of poly(4,4'-biphenylene terephthalate)s substituted with poly(ethylene glycol) side pendants that were employed as polymeric matrices for the preparation of gold nanoparticles.

*e-mail: jijin@korea.ac.kr

1598-5032/04/195-11 ©2004 Polymer Society of Korea

In this study, we investigated LC properties of poly(1,4-phenylene or 4,4'-biphenylene terephthalate) bearing oligo (oxyethylene) side pendants and studied the electrical conductivities of their blends with the lithium salts, LiCF_3SO_3 . Our expectation was that the side pendants would provide channels for carrier transport and the rigid backbone would act as a mechanical strength builder. In the present article their synthesis, thermal analysis, liquid crystalline properties, and ionic conductivities of the lithium salt/polymer complexes will be described.



For the sake of brevity, we call the two polymers **DIPEG-HQ** and **DIPEG-BP**. DiPEG stands for the two PEO ($\text{DP} = 7$, $\text{MW} = 350$) substituents on terephthalate units, and HQ and BP stand for hydroquinone and 4,4'-biphenol moieties in the repeating units in the main chain, respectively.

Experimental

Synthetic route to the polymers are shown in Scheme I. The numbers given in this section for the intermediates and monomer are the same as given in the scheme.

Synthesis of Monomers.

ω -Methoxy poly(ethylene glycol) toluenesulfonate (1): This compound was prepared following the literature method.³²

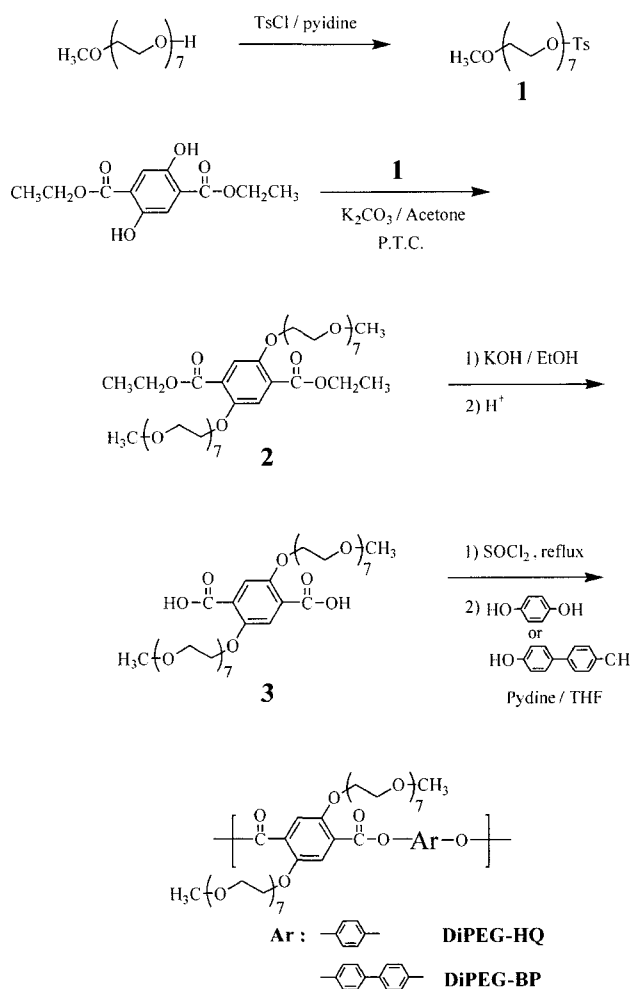
Diethyl 2,5-bis[ω -methoxy-poly(ethylene glycol)] terephthalate (2): Into a 500 mL two-necked round-bottomed flask equipped with a water condenser and an argon gas inlet placed sequentially were acetone (350 mL), anhydrous potassium carbonate (16.0 g), compound **1** (43.6 g; 86.5 mmol) and diethyl 2,5-dihydroxyterephthalate (10.0 g; 39.3 mmol) and flushed with the argon gas. The reaction mixture was heated with stirring to and kept at 65 °C for 24 h. The reaction mixture was cooled to room temperature and the solid formed was collected on a filter and discarded. Acetone in the filtrate was removed by evaporation and then the residue was dissolved in 100 mL of distilled water. And then the temperature was increased to 80 °C, separating the product as precipitate that was collected by centrifuge. This separation method was repeated twice more. This separation method is based on the low critical saturation temperature (LCST)³³ of the product. The oily product was finally purified by column chromatography using a silica gel (60–120 mesh) column. Elution with a mixture of methanol/methylene chloride (v/v

= 1/7) afforded a slightly yellow, oily compound. The LCST of the compound is 53 °C at 10 w% in water; yield: 26.7 g (70%).

IR (KBr, cm^{-1}): 3028 (aromatic C-H stretching), 2915 and 2833 (aliphatic C-H stretchings), 1727 (C=O stretching), 1601 and 1502 (aromatic C=C stretchings), and 1222, 1154, and 955 (C-O stretchings); $^1\text{H-NMR}$ (CDCl_3 , δ_{ppm}): 7.39 (s, 2H, Ar), 4.4~3.5 (m, 66H, $\text{OCH}_2\text{CH}_2\text{O}$, $\text{COOCH}_2\text{CH}_3$, CH_2OCH_3), 1.4 (m, 6H, $\text{COOCH}_2\text{CH}_3$); Elemental analysis, calc. for $\text{C}_{42}\text{H}_{74}\text{O}_{20}$: C 56.11, H 8.30; found C 55.99, H 8.42%.

2,5-Bis[ω -methoxy-poly(ethylene glycol)] terephthalic acid (3): Compound **2** (20.2 g; 22.0 mmol) was dissolved in 250 mL of ethanol containing 12.3 g (0.2 mol) of KOH. The mixture was refluxed for 6 h. The reaction mixture was cooled to room temperature and then the solution was acidified to pH 2 by adding 1 M HCl. After removal of the solvent, the product was separated using the same method as for compound **2**. The LCST of final product was 61 °C at 10 w% in water. Recovered yield of the oily product was 17.0 g (90%).

IR (KBr, cm^{-1}): 3430~2760 (acid OH stretching), 2951



Scheme I. Synthetic route to the monomer and polymers.

and 2782 (aliphatic C-H stretchings), 1701 (acid C=O stretching), 1604 and 1505 (aromatic C=C stretchings), and 1342, 1164, and 993 (C-O stretchings); ¹H-NMR (CDCl₃, δ_{ppm}): 7.8 (s, 2H, Ar), 4.4~3.5 (m, 66H, OCH₂CH₂O, CH₂OCH₃); Elemental analysis, calc. for C₃₈H₆₆O₂₀: C 54.15, H 7.89; found C 54.10, H 7.95%.

Polymer Synthesis.

Two polymers were prepared in the same manner. Therefore, synthetic details are given below only for the preparation of the polymer having the hydroquinone repeating unit, i.e., **DiPEG-HQ** as a representative example. The structures of all the polymers were confirmed by elemental analysis and IR and NMR spectroscopy.

DiPEG-HQ Polymer. Terephthalic acid derivative **3** (3.626 g, 4.20 mmol) was dissolved in 15 mL of thionyl chloride containing 0.1 mL of *N,N*-dimethylformamide. And the mixture was refluxed for 4 h under a dry nitrogen atmosphere. After the excess thionyl chloride was removed by distillation under vacuum, the diacid dichloride formed was dissolved in 18 mL of an ice-chilled mixture of dry tetrahydrofuran (THF) and pyridine (5:2 by vol.) to which added was a solution of hydroquinone (0.463 g, 4.20 mmol) dissolved in 10 mL of dry THF. After being stirred for 20 h, the reaction mixture was poured into excess methanol with vigorous stirring. The precipitate was separated using a centrifuge. The product was purified by dialysis using a cellulose semi-permeable membrane (molecular weight cut-off: 12,000) for 2 days. The polymer thus obtained was dried in a vacuum oven at 50 °C. Yield 2.9 g (75%).

IR (KBr, cm⁻¹): 3033 (aromatic C-H stretching), 2902 and 2787 (aliphatic C-H stretchings), 1724 (C=O stretching), 1604 and 1506 (aromatic C=C stretchings), and 1342, 1150, and 965 (C-O stretchings); ¹H-NMR (CDCl₃, δ_{ppm}): 7.66 (s, 2H, Ar), 7.33 (s, 4H, Ar), 4.4~3.5 (m, 62H, OCH₂CH₂O, CH₂OCH₃); Elemental analysis, calc. for C₄₄H₆₈O₂₀: C 57.63, H 7.47; found C 57.44, H 7.66%.

DiPEG-BP Polymer: This polymer was prepared from **3** and 4,4'-biphenol in the same manner as described above for the preparation of the **DiPEG-HQ** polymer. The recovered yield was 0.91 g (62%).

IR (KBr, cm⁻¹): 3035 (aromatic C-H stretching), 2927 and 2787 (aliphatic C-H stretchings), 1725 (C=O stretching), 1606 and 1504 (aromatic C=C stretchings), and 1338, 1149, and 966 (C-O stretchings); ¹H-NMR (CDCl₃, δ_{ppm}): 7.69 (m, 6H, Ar), 7.33 (m, 4H, Ar), 4.4~3.5 (m, 62H, OCH₂CH₂O, CH₂OCH₃); Elemental analysis, calc. for C₅₀H₇₂O₂₀: C 60.47, H 7.31; found C 60.40, H 7.38%.

Characterization

FT-IR and ¹H-NMR spectra of the intermediates, monomer, and polymers were recorded on a Bomem MB instrument and on a Varian Gemini 300 spectrometer, respectively. Thermal properties were studied in nitrogen atmosphere on

a differential scanning calorimeter (DSC; Mettler DSC 821^c, Germany) at the heating and cooling rate of 10 °C/min. Molecular weight was determined using a DIONEX P580 gel permeation chromatograph equipped with light scattering detector (Wyatt Technology, Down EOS, U.S.A.) and RI detector (OPTI Lab., U.S.A.). Tetrahydrofuran was employed as the eluent and the reference used was polystyrene standard. The phase transitions and optical textures were examined on a polarizing microscope (Olympus BH-2, Japan) equipped with a hot stage (Mettler FP-82HT, Germany) controlled by an automatic thermal controller (Mettler FP-90, Germany). The X-ray diffractograms of the polymers were obtained at varying temperatures using a synchrotron radiation (1.542 Å) of the 3C2 beam line at the Pohang Synchrotron Laboratory, Korea. Ionic conductivity of polymer electrolytes were determined by the impedance method using an IM6 system (Zahner Co., Germany) with a home-made dielectric interface in the frequency range from 100 to 4.0 × 10⁶ Hz. The electrical conductivity was estimated from the measured bulk resistance. The sample temperature was regulated by a water jacket over the temperature range from 20 to 90 °C (±0.5 °C). The conductivity was measured at each temperature after equilibration for 30 min. For sample preparation, the salt, LiCF₃SO₃, was dried at 120 °C for 24 h under vacuum (0.1 torr) and water in the polymers were removed by azeotropic distillation with benzene followed by drying at 45 °C for 24 h under vacuum. And then, polymer/salt mixtures were dissolved in dry THF in a vacuum glove box. The solution was cast on a platinum electrode (14 mm in diameter). After evaporation of the solvent, the films were vacuum dried at 70 °C for at least 20 h. The resulting polymer/salt film thickness was 100 μm. Then, the films were placed in a Teflon cell and glued in a vacuum glove box.

Results and Discussion

Synthesis and General Properties of Polymers. Monomer, **3**, was prepared via a multi-step synthetic route as shown in Scheme I. The structures of the intermediates and monomer were confirmed by elemental and IR and NMR spectroscopy. The two polymers, **DiPEG-HQ** and **DiPEG-BP**, were synthesized by polymerizing the diacid dichloride monomer bearing oligo(oxyethylene) pendants with hydroquinone or 4,4'-biphenol at 60 °C in THF in the presence of pyridine as an HCl-acceptor. Polymerization proceeded homogeneously throughout the polymerization. The resulting polymers were subjected to dialysis using semi-permeable cellulose membrane (molecular weight cut-off: 12,000) using a mixture of methanol and water (2:1) in order to remove soluble impurities and low molecular weight products. The structures of the polymers also were confirmed by elemental analysis and spectroscopic analysis.

The polymers were soluble at room temperature in common organic solvents such as THF, methylene chloride and

Table I. Characteristics of DiPEG-HQ and DiPEG-BP

Polymer	\overline{M}_n^a	\overline{M}_w^a	\overline{PDI}^a	\overline{DP}^a
DiPEG-HQ	30,400	37,700	1.24	31
DiPEG-BP	42,800	59,700	1.40	41

^aThe values were obtained by GPC (DIONEX P580; eluent: THF) using a light scattering detector (Wyatt Technology, Down EOS).

chloroform. Table I summarizes the general properties of the polymers thus obtained. The number average molecular weights (\overline{M}_n) were 30,400 for **DiPEG-HQ** and 42,800 for **DiPEG-BP**. These values correspond to degrees of polymerization of about 31 and 41, respectively. Their average polydispersity indices are 1.24 and 1.40, respectively. Usually, condensation polymerization of diacid dichloride monomer bearing small substituents results in high molecular weight (MW) polymers.^{34,35} In contrast, the monomers having bulky substituents produce relatively low MW polymers, most probably due to steric hindrance in chain growth reactions. We did not attempt to run a high temperature melt polymerization in order to avoid the possible thermal decomposition of the PEG pendants during the course of polymerization.

Liquid Crystalline Properties. An investigation of phase transitions of the bulk polymers was carried out by DSC and X-ray diffractometry. In order to exclude any possible artifacts arising from different sample history, both polymers were first heated to 200°C and then cooled to -60°C at the cooling rate of 10°C/min.

As shown in DSC thermograms of **DiPEG-HQ** (Figure 1), two small peaks at -31 and 35°C, were observed on both heating and cooling curves. **DiPEG-BP**, however, exhibits three endothermic peaks at -35, 66 and 143°C on the heating cycle. The transitions were reversible as one can see from the corresponding cooling DSC thermogram; three corresponding exothermic peaks appeared on the cooling cycle.

When we examined the optical textures of the two polymers, **DiPEG-HQ** revealed only a very weak birefringence below

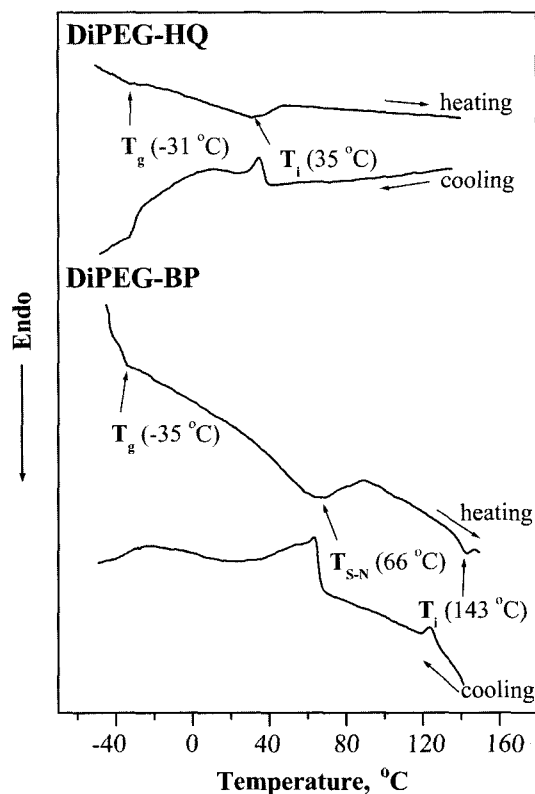


Figure 1. DSC thermograms of **DiPEG-HQ** and **DiPEG-BP** obtained under a nitrogen atmosphere at the heating and cooling rates of 10°C/min.

35°C (Figure 2). And this weak birefringence disappeared at 47°C. In contrast, **DiPEG-BP** exhibits a broken marble texture at room temperature, and with increasing the temperature, the so-called polished marble texture typical of nematic liquid crystals is observed up to 143°C (Figure 2).

Combination of the microscopic observation and DSC and X-ray analyses to be described below, leads to the conclusion that the mesophase formed by the two polymers is of a layered morphology at room temperature. The two polymers

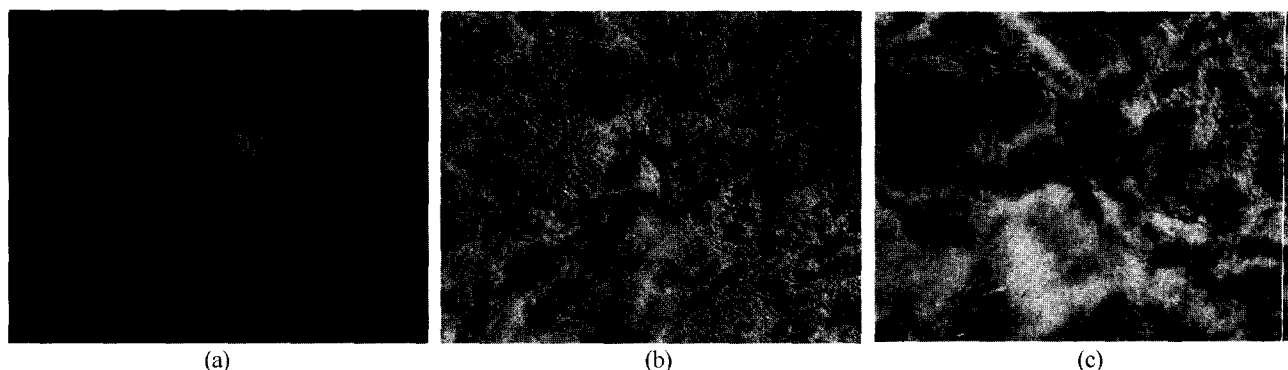


Figure 2. Optical photomicrograph of (a) **DiPEG-HQ** taken at 32°C, (b) **DiPEG-BP** taken at 30°C, and (c) at 110°C (magnification 200×).

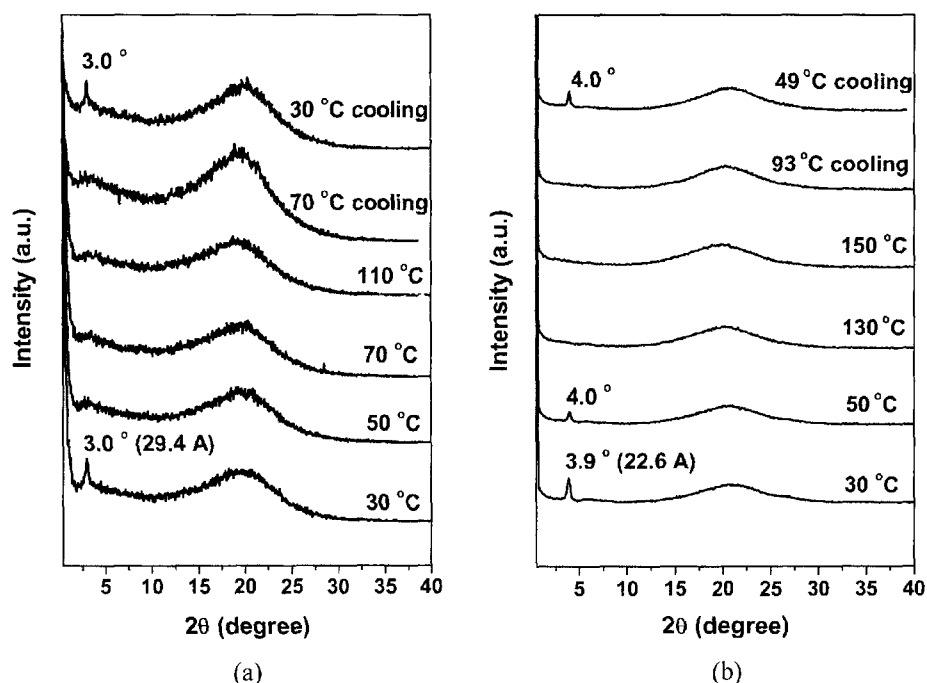


Figure 3. Wide angle X-ray diffractograms of (a) **DiPEG-HQ** and (b) **DiPEG-BP**.

glass transition temperatures are -31 and -35°C , respectively (Figure 1). In the case of **DiPEG-BP**, the second peak represents a layered structure \rightarrow nematic mesophase transition, while the third peak is associated with isotropization. But **DiPEG-HQ** reveals a direct transition from a layered structure to the isotropic state.

According to Figure 3, the two polymers commonly show one sharp diffractogram peak at room temperature in the small angle region. The long spacings estimated from the diffraction angle $2\theta = 3.0^\circ$ and 3.9° , are 29.4 and 22.6 \AA , respectively for **DiPEG-HQ** and **DiPEG-BP**. The wide angle X-ray diffractograms shown in Figure 3 tell us that the two polymers form fluid mesophases in the light of the broad diffractions at $2\theta = 15\text{--}22^\circ$ ($5.9\text{--}4.4 \text{ \AA}$) that correspond to short spacing, or interchain distance.

The only structural difference between **DiPEG-HQ** and **DiPEG-BP** lies in the fact that the phenylene ring in the backbone mesogenic group of the former has been replaced with the biphenylene group in the latter. The biphenylene group is expected to increase the length of the rigid backbone repeating unit. The **DiPEG-BP** polymer having a longer, rigid repeating unit, exhibits both layered and nematic structures, whereas **DiPEG-HQ** polymer having a shorter one only a layered structure. In addition, the distance (29.4 \AA) between the polymer backbones for **DiPEG-HQ** is greater than that (22.6 \AA) of **DiPEG-BP**, since the shorter length of the repeating unit requires more lateral space to accommodate the side pendants. Based on these X-ray analyses, we propose that the mesophases of **DiPEG-HQ** and **DiPEG-BP** have

layered structures at room temperature as shown in Figure 4. The polymer main chains are packed parallel to each other, and the side groups occupy the space between the layers. The hydrophobic nature of the backbone and the hydrophilic character of the side pendants, or disparity in hydro- or lyophilicity of the backbone and the pendants appear to favor the formation of a smecticlike layered morphology in the mesophase.

One important question one may raise is how the smectic layer spacing would change as one mix the polymers with the lithium salt. We found that the layer spacing of the polymer electrolyte composites was found to increase with increasing amount of the lithium salt as demonstrated by the small angle diffractograms (Figure 5) obtained at room temperature. Figure 5(a) shows the long spacing steadily increases from 29.4 \AA ($2\theta = 3.0^\circ$) for the virgin, uncomplexed polymer of **DiPEG-HQ** to 33.6 \AA ($2\theta = 2.63^\circ$) when the concentration ratio of $[\text{EO}]/[\text{Li}^+] = 5$. The exact same trend is observed for **DiPEG-BP/LiCF₃SO₃** composites; the long spacing increases from 22.6 \AA ($2\theta = 3.9^\circ$) of the virgin polymer to 26.0 \AA ($2\theta = 3.40^\circ$) for the **DiPEG-BP/LiCF₃SO₃** composite when $[\text{EO}]/[\text{Li}^+] = 5$. Evidently, complexation of the oligo(oxyethylene) pendants with the lithium salt molecules expands the space originally occupied by the pendants and, thus increases the molecular breath or the interlayer distance in the smectic LC morphology. In other words, the salt swells the oligo(oxyethylene) domain in the LC state.

The phase transition behavior of the two polymers also exhibits a noticeable dependence on the salt concentration.

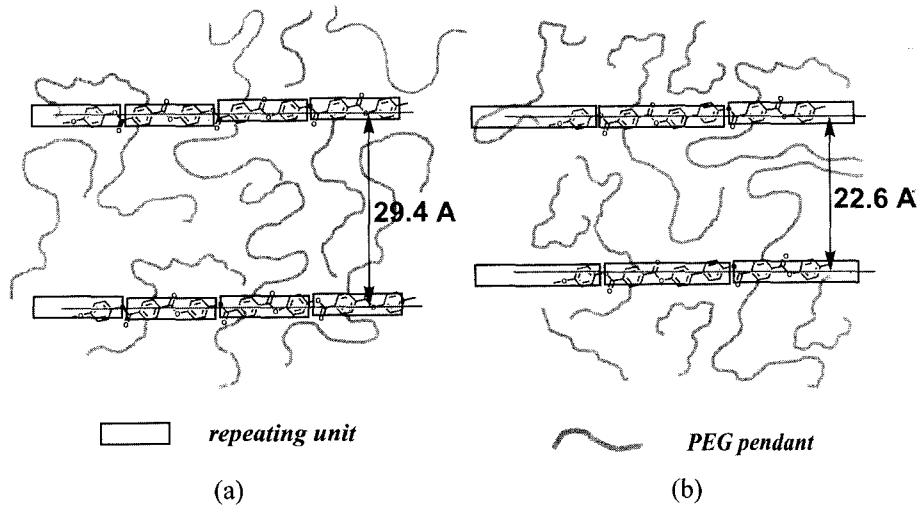


Figure 4. Proposed layer structure of (a) DiPEG-HQ and (b) DiPEG-BP.

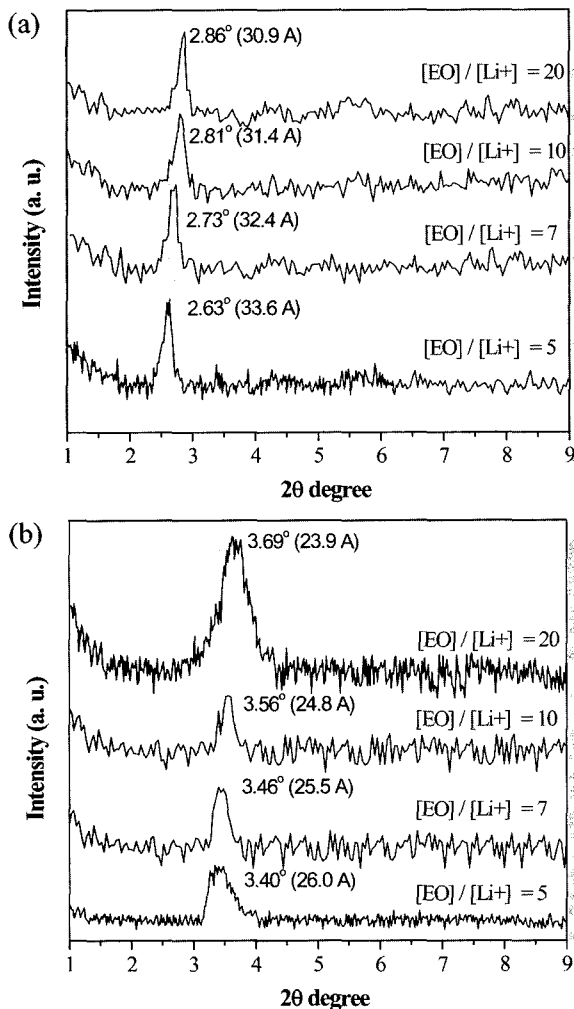


Figure 5. Small angle X-ray diffractograms at room temperature for (a) DiPEG-HQ/LiCF₃SO₃ and (b) DiPEG-BP/LiCF₃SO₃ composites containing various LiCF₃SO₃ concentrations.

Figure 6 compares the DSC thermograms of DiPEG-BP/LiCF₃SO₃ complexes containing different levels of the salt. There are a couple of importance points to note: The T_g value is elevated from -35 to -25 °C with increasing the salt content^{29,39} in the mixture and the S→N transition temperature also steadily increases from 66 °C for the original polymer to 106 °C for the DiPEG-BP/LiCF₃SO₃ composite having the ratio of [EO]/[Li⁺] = 5. This can be ascribed to an augmentation of chain stiffness by complex formation between the salt and the PEG pendants. At the same time, the nematic phase observed for the original polymer slowly disappears as we increase the salt content; when [EO]/[Li⁺] = 20, the nematic phase still appeared, which is clearly discernible on the top DSC thermogram in Figure 6. The phase, however, is barely observed when we increased the salt content further to [EO]/[Li⁺] = 10 and 7. The composition of [EO]/[Li⁺] = 5 did not form the nematic phase, which could be confirmed both by DSC analysis and polarizing microscopy. The same trend was observed also for DiPEG-HQ/LiCF₃SO₃ mixtures. The S→I transition temperature steadily increases from 35 °C for the original polymer to 71 °C for the DiPEG-HQ/LiCF₃SO₃ composite having the ratio of [EO]/[Li⁺] = 5. The T_g values of DiPEG-HQ/salt mixtures, however, could not be determined unequivocally by DSC analysis.

FT-IR Spectroscopy and Ionic Conductivity Properties. FT-IR spectroscopy is a powerful tool for probing microscopic details in electrolytic system containing LiCF₃SO₃. In particular, the characteristic $\nu_s(\text{SO}_3^-)$ internal vibrational modes of the CF₃SO₃⁻ anion are sensitive to the change in the local anionic environment. According to literature,³⁶⁻³⁹ the component observed at about 1032 cm⁻¹ has been assigned to the free anions which do not interact directly with lithium cations. Components at about 1042 and 1050-1054 cm⁻¹ have been attributed to contact ion pairs and Li₂CF₃SO₃⁺ triple ions or ionic aggregates, respectively.

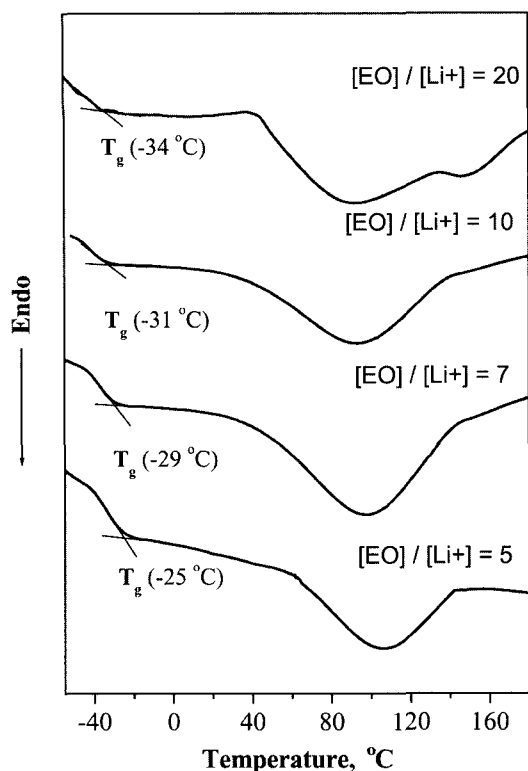


Figure 6. DSC thermograms of **DiPEG-BP**/LiCF₃SO₃ composite electrolyte containing various LiCF₃SO₃ concentrations obtained under a nitrogen atmosphere at the heating and cooling rates of 10 °C/min.

Figure 7 shows typical IR spectra in the $\nu_s(\text{SO}_3)$ spectral region of **DiPEG-HQ** from 1010 to 1070 cm⁻¹ at room temperature for varying ratios of the ethylene oxide (EO) repeating unit/Li⁺ ion. Fractions of the free anions, ionic pairs

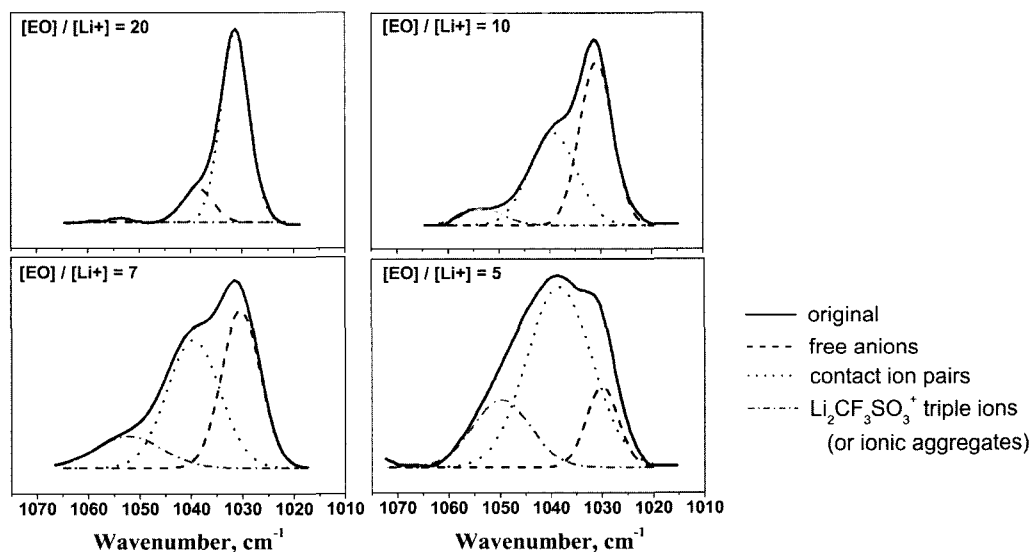


Figure 7. Infrared spectra of the $\nu_s(\text{SO}_3)$ internal modes for **DiPEG-HQ**/LiCF₃SO₃ composite electrolyte.

and ionic aggregates of the electrolyte are measured by decomposition of the $\nu_s(\text{SO}_3)$ band into three Gaussian peaks. A similar analysis can be performed for the LiCF₃SO₃-doped **DiPEG-BP**, although its IR spectra are not given. The results of curve fitting are summarized in Table II for **DiPEG-HQ** and **DiPEG-BP**, where one can see that the fraction of free anions increases with increase in the [EO]/[Li⁺] ratio in both systems. And formation of ionic aggregates is not observed at lower [EO]/[Li⁺] ratio, but it rapidly increases with decrease in the [EO]/[Li⁺] ratio.³⁹⁻⁴¹

The ionic conductivity was measured for the polymer/Li⁺ composite samples sandwiched between two platinum plates under inert atmosphere. The ionic conductivity values of the samples were calculated by the following equation :

$$\sigma = (1/R_B)d/S \quad (1)$$

where σ is the ionic conductivity, d the thickness of the sample, S the area of the Pt electrode, and R_B the bulk resistance of the sample. AC impedance was measured to determine the conductivity (σ) of these films. The impedance values were obtained by the Cole-Cole plot⁴²⁻⁴⁴ of the resistance against various frequencies.

The temperature dependence of the ion conductivity (σ) was evaluated by impedance spectroscopy over the temperature range of 25~90 °C. Figure 8 shows the dependence of conductivity of **DiPEG-HQ** and **DiPEG-BP** complexes on the LiCF₃SO₃ concentration at different temperatures. All complexes exhibit a similar trend : increasing the salt concentration resulted in an increase in the ionic conductivity as a result of increasing number of charge carriers. The increase in conductivity, however, was less than one order of magnitude due to the formation of ion pairs and aggregates that reduce the charge mobility.^{29,45}

Table II. Curve-fitting Data of Infrared Spectra of Symmetric SO_3 Stretching Mode, $\nu_s(\text{SO}_3)$, for PEO-based Electrolyte Composites at Various $[\text{EO}]/[\text{Li}^+]$ Mole Ratio^a

[EO]/[Li ⁺] Mole Ratio	DiPEG-HQ			DiPEG-BP		
	Free (mole %)	Pairs (mole %)	Aggr. (mole %)	Free (mole %)	Pairs (mole %)	Aggr. (mole %)
20	83.2	14.4	1.4	81.1	15.2	3.7
10	57.5	37.8	4.7	67.3	27.0	5.7
7	40.3	45.7	14.0	45.7	46.1	9.2
5	30.0	53.9	16.1	38.0	47.2	14.8

^aThe characteristic $\nu_s(\text{SO}_3)$ internal mode of the CF_3SO_3^- anion is sensitive in changing the local anionic environment. The components observed at ~ 1032 , ~ 1042 and ~ 1050 - 1054 cm^{-1} have been attributed to free anion, contact ion pairs and $\text{Li}_2\text{CF}_3\text{SO}_3^+$ triple ions (or ionic aggregates), respectively.

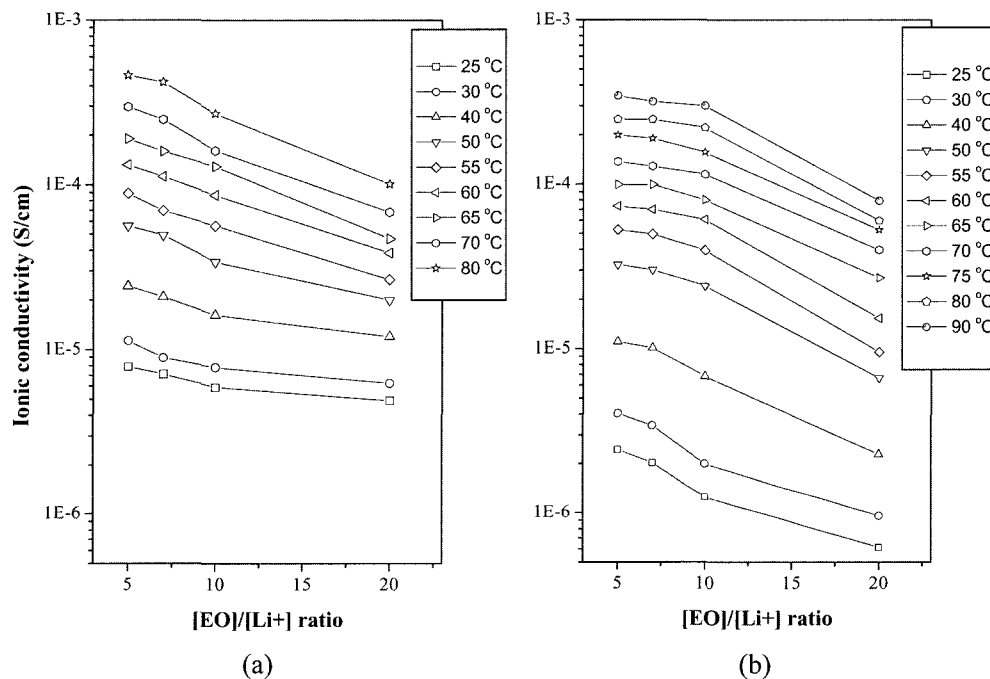
**Figure 8.** Variation of conductivity of (a) **DiPEG-HQ** and (b) **DiPEG-BP** electrolyte with LiCF_3SO_3 concentration at different temperature.

Figure 9 illustrates Arrhenius conductivity plots for the polymer electrolytes at various Li^+ ion concentrations. It is evident that the temperature dependence of conductivity is not perfectly linear, which is in line with earlier observations made by other researchers. Moreover, it should be pointed out that the present polymers undergo phase changes in the temperature range examined in this study.^{46,49}

The activation energy (E_a) of conductivity for various Li ion concentrations was calculated from the Arrhenius equation

$$\sigma = \sigma_0 \exp(-E_a/RT) \quad (2)$$

where T is temperature in the Kelvin scale, σ_0 a proportional constant and R a Boltzman constant. Since the two polymers start to undergo phase transitions (Figure 6) at relatively low temperature when mixed with various amount of the salt, the activation energy (E_a) for conductivity was estimated only with the data obtained up to 40°C for **DiPEG-HQ** and up to 50°C for **DiPEG-BP**. In fact, we note that the Arrhenius plots look much more linear over the lower temperature regime than over the higher temperature regime. In the higher temperature regime, the mixtures are undergoing phase transitions, which may be an important reason why we do not attain better linear plots.

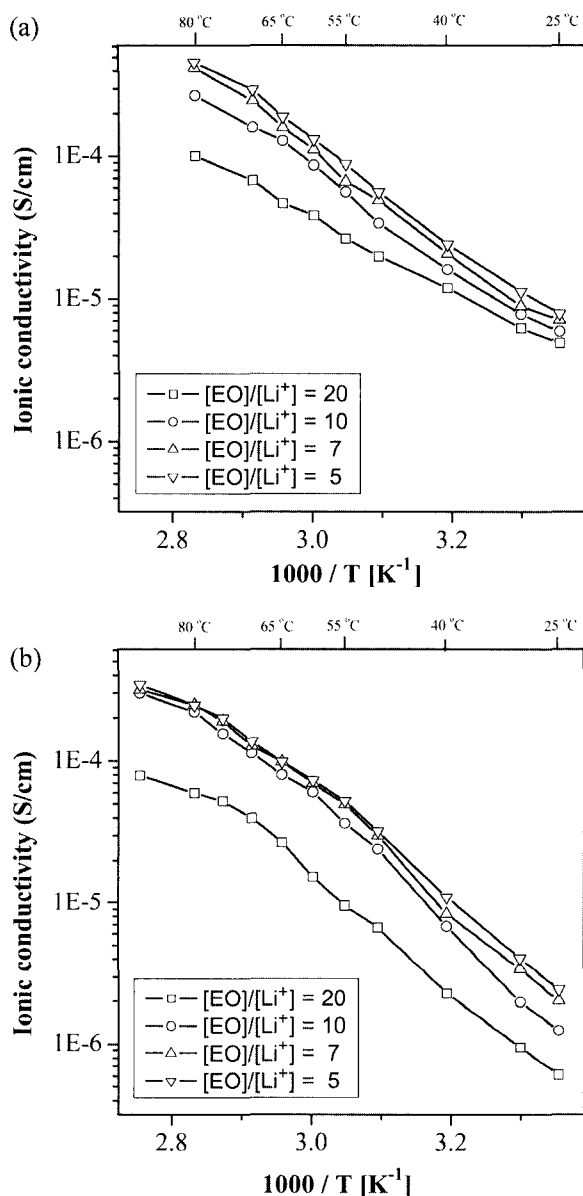


Figure 9. Arrhenius conductivity plots for (a) **DiPEG-HQ**/ LiCF_3SO_3 and (b) **DiPEG-BP**/ LiCF_3SO_3 composite electrolyte containing various LiCF_3SO_3 concentrations.

Table III compares the E_a values of the composites of the two polymers at various salt content. There are three interesting points to be emphasized: (1) The E_a values of the **DiPEG-HQ** composites are higher than those of the **DiPEG-BP** composites. The higher rigidity of the latter appears to be a reason for this difference. (2) The E_a value increases with increasing salt concentration. This phenomenon was also observed earlier by others.^{50,51} (3) And the E_a values are not much different from those of the composites prepared from other polymers bearing PEG pendants.^{51,52} The values, however, are significantly higher than those reported for PEG-salt mixtures. They usually range from 0.1 to 0.3 eV.^{49,53}

Table III. Activation Energy for the Conductivity of Composites at Various $[\text{EO}]/[\text{Li}^+]$ Mole Ratio

		Layered Structures	
		Activation Energy (eV)	Activation Energy (Kcal/mol)
DiPEG-HQ/Li	20	0.48 (± 0.04)	9.5 (± 0.8)
	10	0.54 (± 0.03)	10.7 (± 0.6)
	7	0.59 (± 0.03)	11.7 (± 0.6)
	5	0.65 (± 0.02)	12.9 (± 0.4)
DiPEG-BP/Li	20	0.78 (± 0.04)	15.4 (± 0.8)
	10	0.87 (± 0.05)	17.2 (± 1.0)
	7	0.87 (± 0.06)	17.2 (± 1.0)
	5	0.88 (± 0.03)	17.4 (± 0.6)

Evidently, electrical conductivity of present type composites is more sensitive to temperature changes due to thermal activation of polymer chain motions which couple with thermal acceleration of ions mobility. The E_a values of the present composites agree well with literature data for similar polymer electrolytes that consist of a stiff main chain with oligo(oxyethylene) side pendants.³⁰

The conductivity values at 40 °C are 2.4×10^{-5} and 1.1×10^{-5} S/cm for **DiPEG-HQ** and **DiPEG-BP**, respectively, at the $[\text{EO}]/[\text{Li}^+]$ ratio of 5. And at 80 °C, the values increase to 4.6×10^{-4} and 2.5×10^{-4} S/cm, respectively. The comparative lower T_g and larger layer spacing of **DiPEG-HQ** appear to result in a higher conductivity when compared with **DiPEG-BP**. In addition, **DiPEG-HQ** exists in the isotropic liquid state at upper 60 °C, but **DiPEG-BP** is in the nematic liquid crystal state. The conductivity values for the present polymer/ Li^+ ion complexes are significantly higher, more than 10 times, than those reported for poly(ethylene oxide) electrolytes. Wegner *et al.*³⁰ reported the conductivity value as high as 1.4×10^{-6} S/cm at room temperature for a poly(*p*-phenylene) having oligo(oxyethylene) side pendants.

Conclusions

We have described the synthesis, LC properties and ionic electrical conductivities of new main chain aromatic polyesters bearing oligo(oxyethylene) pendants. The **DiPEG-BP** polymer having a longer repeating unit exhibits both layered and nematic mesophases, whereas **DiPEG-HQ** polymer having a shorter repeating unit shows only the layered morphology in mesophase. Both polymers easily form complexes with LiCF_3SO_3 . The composites containing the salt exhibited increased layer spacing when compared with uncomplexed polymers. Electrical conductivities of polymer/ Li^+ ion composites are about $1.1 \sim 2.4 \times 10^{-5}$ S/cm at 40 °C, which are considered to be reasonably high. Increasing the length of the poly(ethylene oxide) pendants and changing the alkali metal salts are expected to enhance their conductivities even

further. Although the layered morphology of the present composites may contribute to the electrical conductivity, it could not be quantitatively evaluated because it is expected that layer morphology must be of liquid crystalline domains. Orientation of the polymer main chains is expected to form oligo(oxyethylene)-salt complex channels that should help ions mobilities resulting in higher conductivities. This aspect should be investigated in future.

Acknowledgements. This research was supported by the Korea Science and Engineering Foundation through the Center for Electro- and Photo-Responsive Molecules, Korea University.

References

- (1) M. Shilata, T. Kokayashi, R. Yosomiya, and M. Seki, *Eurp. Polym. J.*, **36**, 85 (2000).
- (2) L. Wang, B. Yang, X. L. Wang, and X. Z. Tang, *J. Appl. Polym. Sci.*, **71**, 1711 (1999).
- (3) T. Noda, S. Kato, Y. Yoshihisa, K. Takeuchi, and K. Murata, *J. Power Sources*, **43-44**, 89 (1993).
- (4) O. Bohnke, C. Rousselot, P. A. Gillet, and C. Truche, *J. Electrochem. Soc.*, **139**, 1862 (1992).
- (5) M. Inaba, Z. Ogumi, and Z. Takehara, *J. Electrochem. Soc.*, **141**, 2579 (1994).
- (6) M. Armand, *Ann. Rev. Mater. Sci.*, **16**, 254 (1986).
- (7) C. A. Angell, *Ann. Rev. Phys. Chem.*, **43**, 693 (1992).
- (8) M. Armand, J. Y. Sanchez, M. Gauthier, and Y. Choquette, in *Electrochemistry of Novel Materials*, J. Lipkowski and P. N. Ross, Eds., VCH Publishers, New York, 1994.
- (9) M. Gauthier, A. Belanger, B. Kapfer, G. Vassort, and M. Armand, in *Polymer Electrolyte Reviews*, J. R. Mac Callum and C. A. Vincent, Eds., Elsevier Applied Science, London, 1989, vol. 2.
- (10) K. M. Abraham, *Electrochim. Acta.*, **38**, 1233 (1993).
- (11) (a) P. V. Wright, *Br. Polym.*, **7**, 319 (1975), (b) P. G. Hall, G. R. Davies, J. E. McIntyre, I. M. Ward, D. J. Banister, and K. M. F. Le Brocq, *Polym. Commun.*, **27**, 98 (1986).
- (12) M. Armand, J. M. Chabagno, and M. Duclot, in *Fast Ion Transport in Solids*, P. Vashishta, Ed., North-Holland, New York, 1979, p. 131.
- (13) M. Watanabe, K. Sanui, N. Ogata, F. Inoue, T. Kobayashi, and Z. Ohtaki, *Polym. J.*, **17**, 549 (1985).
- (14) J. R. M. Ailes, F. M. Gray, J. R. Mac Callum, and C. A. Vincent, *Polymer*, **28**, 1977 (1989).
- (15) M. Nekoomanesh, H. S. Nagae, C. Booth, and J. R. Owen, *J. Electrochem. Soc.*, **139**, 3046 (1992).
- (16) R. Borkowska, J. Laskowski, J. Plochanski, J. Przyluski, and W. Wiczorek, *J. Appl. Electrochem.*, **23**, 991 (1993).
- (17) E. Quartarone, P. Mustarelli, and A. Magistris, *Solid State Ionics*, **110**, 2251 (1995).
- (18) K. M. Abraham, Z. Jiang, and B. Carroll, *Chem. Mater.*, **9**, 1978 (1997).
- (19) Y.-W. Park and D.-S. Lee, *Polymer(Korea)*, **27**, 265 (2003).
- (20) W. Wiczorek and J. R. Stevens, *J. Phys. Chem. B.*, **101**, 1529 (1997).
- (21) C. Booth, C. V. Nicolas, and D. J. Wilson, in *Polymer Electrolyte Reviews*, J. R. Mac Callum and C. A. Vincent, Eds., Elsevier Applied Science, London, 1989, vol. 2, p. 229.
- (22) M. Kono, E. Hayashi, and M. Watanabe, *J. Electrochem. Soc.*, **145**, 1521 (1998).
- (23) P. M. Blonsky, D. F. Shriver, P. Austin, and H. R. Allcock, *J. Am. Chem. Soc.*, **106**, 6854 (1984).
- (24) R. A. Reed, T. T. Wooster, R. W. Murray, D. R. Vaniv, J. S. Tonge, and D. F. Shriver, *J. Electrochem. Soc.*, **136**, 2565 (1989).
- (25) Y. Heo, Y. Kang, K. Han, and C. Lee, *Polymer(Korea)*, **27**, 385 (2003).
- (26) I. M. Ward, J. E. McIntyre, G. R. Davies, S. A. Dobrowski, S. R. Mirrezaei, and H. V. St. A. Hubbard, *Electrochim. Acta.*, **37**, 1479 (1992).
- (27) H. V. St. A. Hubbard, S. A. Sills, G. R. Davis, J. E. McIntyre, and I. M. Ward, *Electrochim. Acta.*, **43**, 1239 (1998).
- (28) F. B. Dias, S. V. Batty, A. Gupta, G. Ungar, J. P. Voss, and P. V. Wright, *Electrochim. Acta.*, **43**, 1217 (1998).
- (29) M. K. Park, J. Kim, and J. Y. Bae, *Electrochem. Commun.*, **3**, 28 (2001).
- (30) U. Lauter, W. H. Meyer, and G. Wenger, *Macromolecules*, **30**, 2092 (1997).
- (31) J.-W. Lee and J.-I. Jin, *J. Nanosci. and Nanotech.*, **3**, 219 (2003).
- (32) R. Hooper, L. J. Lyons, M. K. Mapes, D. Schumacher, D. A. Moline, and R. West, *Macromolecules*, **34**, 931 (2001).
- (33) S.-B. Lee, S.-C. Song, Y.-S. Sohn, and J.-I. Jin, *Macromolecules*, **34**, 7565 (2001).
- (34) H. R. Kricheldorf and D. F. Wulff, *Polymer*, **39**, 2681 (1998).
- (35) J. Watanabe, N. Sekine, T. Nematsu, M. Sone, and H. R. Kricheldorf, *Macromolecules*, **29**, 4816 (1996).
- (36) W. Haung, R. Frech, and R. A. Wheeler, *J. Phys. Chem.*, **98**, 100 (1994).
- (37) A. Ferry, *J. Phys. Chem. B*, **101**, 150 (1997).
- (38) A. Ferry, G. Orädd, and P. Jacobsson, *J. Chem. Phys.*, **108**, 7426 (1998).
- (39) M. Digar, S. L. Hung, H. L. Wang, T. C. Wen, and A. Gopalan, *Polymer*, **43**, 681 (2002).
- (40) H.-W. Chen and F.-C. Chang, *Polymer*, **42**, 9763 (2001).
- (41) P. Jannasch, *Polymer*, **42**, 8629 (2001).
- (42) Y.-T. Cheng and T.-C. Wen, *Solid State Ionics*, **107**, 161 (1998).
- (43) T.-T. Cheng and T.-C. Wen, *J. Electroanal. Chem.*, **459**, 99 (1998).
- (44) J. Y. Song, Y. Y. Wang, and C. C. Wan, *J. Power Sources*, **77**, 183 (1999).
- (45) T.-C. Wen, Y.-J. Wang, T.-T. Cheng, and C.-H. Yang, *Polymer*, **40**, 3979 (1999).
- (46) M. Watanabe, K. Sanui, and N. Ogata, *Macromolecules*, **19**, 815 (1986).
- (47) J. D. van Heumen and J. R. Stevens, *Macromolecules*, **28**, 4268 (1995).
- (48) T. Sreekanth, M. J. Reddy, S. Subramanyam, and U. V. Subba Rao, *Mater. Sci. Eng.*, **B64**, 107 (1999).
- (49) P. P. Chu, M. J. Reddy, and H. M. Kao, *Solid State Ionics*, **156**, 141 (2003).
- (50) T. Sreekanth, M. Jaipal Reddy, S. Subramanyam, and U. V.

Subba Rao, *Mater. Sci. Eng.*, **B64**, 107 (1999).

(51) T. J. Cleij, L. W. Jenneskens, M. Wübbenhorst, and J. van Turnhout, *Macromolecules*, **32**, 8663 (1999).

(52) J.-L. Qiao, N. Yoshimoto, M. Ishikawa, and M. Morita, *Elec-*

trochimica Acta., **47**, 3441 (2002).

(53) J. Castillo, I. Delgado, M. Chacón, and R. A. Vargas, *Electrochimica Acta.*, **46**, 1695 (2001).